PHYSICAL REVIEW D **85,** 112013 (2012)

Measurement of the ratio of branching fractions $\mathcal{B}(B^0 \to K^{*0}\gamma)/\mathcal{B}(B_s^0 \to \phi\gamma)$

R. Aaij *et al.**
(LHCb Collaboration)

(Received 1 March 2012; published 25 June 2012)

The ratio of branching fractions of the radiative B decays $B^0 \to K^{*0}\gamma$ and $B^0 s \to \phi\gamma$ has been measured using 0.37 fb^{-1} of pp collisions at a center of mass energy of $\sqrt{s} = 7$ TeV, collected by the LHCb experiment. The value obtained is $\frac{\mathcal{B}(B^0 \to K^{*0}\gamma)}{\mathcal{B}(B^0 s \to \phi\gamma)} = 1.12 \pm 0.08^{+0.06+0.09}_{-0.04-0.08}$, where the first uncertainty is statistical, the second systematic, and the third is associated with the ratio of fragmentation fractions f_s/f_d. Using the world average for $\mathcal{B}(B^0 \to K^{*0}\gamma) = (4.33 \pm 0.15) \times 10^{-5}$, the branching fraction $\mathcal{B}(B^0 s \to \phi\gamma)$ is measured to be $(3.9 \pm 0.5) \times 10^{-5}$, which is the most precise measurement to date.

DOI: 10.1103/PhysRevD.85.112013 PACS numbers: 13.40.Hq, 13.20.He

I. INTRODUCTION

In the standard model (SM) the decays $B^0 \to K^{*0}\gamma$ and $B_s^0 \to \phi\gamma$[1] proceed at leading order through $b \to s\gamma$ one-loop electromagnetic penguin transitions, dominated by a virtual intermediate top-quark coupling to a W boson. Extensions of the SM predict additional one-loop contributions that can introduce sizeable effects on the dynamics of the transition [1].

Radiative decays of the B^0 meson were first observed by the CLEO Collaboration in 1993 [2] through the decay mode $B \to K^*\gamma$. In 2007, the Belle Collaboration reported the first observation of the analogous decay in the B_s^0 sector, $B_s^0 \to \phi\gamma$ [3]. The current world averages of the branching fractions of $B^0 \to K^{*0}\gamma$ and $B_s^0 \to \phi\gamma$ are $(4.33 \pm 0.15) \times 10^{-5}$ and $(5.7^{+2.1}_{-1.8}) \times 10^{-5}$, respectively [4,5]. These results are in agreement with the latest SM theoretical predictions from next-to-leading-order calculations using SCET [6], $\mathcal{B}(B^0 \to K^{*0}\gamma) = (4.3 \pm 1.4) \times 10^{-5}$ and $\mathcal{B}(B_s^0 \to \phi\gamma) = (4.3 \pm 1.4) \times 10^{-5}$, which suffer from large hadronic uncertainties. The ratio of experimental branching fractions is measured to be $\mathcal{B}(B^0 \to K^{*0}\gamma)/\mathcal{B}(B_s^0 \to \phi\gamma) = 0.7 \pm 0.3$, in agreement with the prediction of 1.0 ± 0.2 [6].

This paper presents a measurement of $\mathcal{B}(B^0 \to K^{*0}\gamma)/\mathcal{B}(B_s^0 \to \phi\gamma)$ using a strategy that ensures the cancellation of most of the systematic uncertainties affecting the measurement of the individual branching fractions. The measured ratio is used to determine $\mathcal{B}(B_s^0 \to \phi\gamma)$, assuming the world average value of $\mathcal{B}(B^0 \to K^{*0}\gamma)$ [4].

II. THE LHCB DETECTOR AND DATASET

The LHCb detector [7] is a single-arm forward spectrometer covering the pseudorapidity range $2 < \eta < 5$, designed for the study of particles containing b or c quarks. The detector includes a high-precision tracking system consisting of a silicon-strip vertex detector surrounding the pp interaction region, a large-area silicon-strip detector located upstream of a dipole magnet with a bending power of about 4 Tm, and three stations of silicon-strip detectors and straw drift-tubes placed downstream. The combined tracking system has a momentum resolution $\Delta p/p$ that varies from 0.4% at 5 GeV/c to 0.6% at 100 GeV/c, and an impact parameter (IP) resolution of 20 μm for tracks with high transverse momentum. Charged hadrons are identified using two ring-imaging Cherenkov detectors. Photon, electron, and hadron candidates are identified by a calorimeter system consisting of scintillating-pad and preshower detectors, an electromagnetic calorimeter (ECAL), and a hadronic calorimeter. Muons are identified by a muon system composed of alternating layers of iron and multiwire proportional chambers. The trigger consists of a hardware stage, based on information from the calorimeter and muon systems, followed by a software stage running on a large farm of commercial processors, which applies a full-event reconstruction.

The data used for this analysis correspond to 0.37 fb^{-1} of pp collisions collected in the first half of 2011 at the LHC with a center of mass energy of $\sqrt{s} = 7$ TeV. $B^0 \to K^{*0}\gamma$ and $B_s^0 \to \phi\gamma$ candidates are required to have triggered on the signal photon and vector-meson daughters, following a definite trigger path. The hardware level must have been triggered by an ECAL candidate with $E_T > 2.5$ GeV. In the software trigger, the events are selected when a track is reconstructed with IP $\chi^2 > 16$, and either $p_T > 1.7$ GeV/c when the photon has $E_T > 2.5$ GeV or $p_T > 1.2$ GeV/c when the photon has $E_T > 4.2$ GeV. The selected track must form a K^{*0} or ϕ candidate when combined with an additional track, and the invariant mass of the combination of the $K^{*0}(\phi)$ candidate and the

*Full author list given at the end of the article.

[1]Charge conjugated modes are implicitly included throughout the paper.

photon candidate is required to lie within a 1 GeV/c^2 window around the nominal $B^0(B_s^0)$ mass.

Large samples (30 times bigger than the data) of $B^0 \to K^{*0}\gamma$ and $B_s^0 \to \phi\gamma$ Monte Carlo (MC) simulated events [8] are used to optimize the signal selection and to parametrize the B-meson invariant mass distribution. The pp collisions are generated with PYTHIA 6.4 [9] and decays of hadronic particles are simulated using EVTGEN [10] in which final-state radiation is generated using PHOTOS [11]. The interaction of the generated particles with the detector and its response are simulated using GEANT4 [12].

III. EVENT SELECTION

The selection of both B decays is designed to ensure the cancellation of systematic uncertainties in the ratio of their efficiencies. The procedure and requirements are kept as similar as possible: the $B^0(B_s^0)$ mesons are reconstructed from a selected $K^{*0}(\phi)$, composed of oppositely charged kaon-pion (kaon-kaon) pairs, combined with a photon.

The two tracks from the vector-meson daughters are both required to have $p_{\rm T} > 500$ MeV/c and to point away from all pp interaction vertices by requiring IP $\chi^2 > 25$. The identification of the kaon and pion tracks is made by applying cuts to the particle identification (PID) provided by the ring-imaging Cherenkov system. The PID is based on the comparison between two particle hypotheses, and it is represented by the difference in logarithms of the likelihoods (DLL) between the two hypotheses. Kaons are required to have $\mathrm{DLL}_{K\pi} > 5$ and $\mathrm{DLL}_{Kp} > 2$, while pions are required to have $\mathrm{DLL}_{K\pi} < 0$. With these cuts, kaons (pions) coming from the studied channels are identified with a $\sim$70(83)% efficiency for a $\sim$3(2)% pion (kaon) contamination.

Two-track combinations are accepted as $K^{*0}(\phi)$ candidates if they form a vertex with $\chi^2 < 9$ and their invariant mass lies within a $\pm 50(\pm 10)$ MeV/c^2 mass window of the nominal $K^{*0}(\phi)$ mass. The resulting vector-meson candidate is combined with a photon of $E_{\rm T} > 2.6$ GeV. Neutral and charged electromagnetic clusters in the ECAL are separated based on their compatibility with extrapolated tracks [13] while photon and π^0 deposits are identified on the basis of the shape of the electromagnetic shower in the ECAL. The B candidate invariant mass resolution, dominated by the photon contribution, is about 100 MeV/c^2 for the decays presented in this paper.

The B candidates are required to have an invariant mass within a ± 800 MeV/c^2 window around the corresponding B hadron mass, to have $p_{\rm T} > 3$ GeV/c, and to point to a pp interaction vertex by requiring IP $\chi^2 < 9$. The distribution of the helicity angle $\theta_{\rm H}$, defined as the angle between the momentum of either of the daughters of the vector meson (V) and the momentum of the B candidate in the rest frame of the vector meson, is expected to follow $\sin^2\theta_{\rm H}$ for $B \to V\gamma$, and $\cos^2\theta_{\rm H}$ for the $B \to V\pi^0$ background. Therefore, the helicity structure imposed by the signal decays is exploited to remove $B \to V\pi^0$ background, in which the neutral pion is misidentified as a photon, by requiring that $|\cos\theta_{\rm H}| < 0.8$. Background coming from partially reconstructed b hadron decays is rejected by requiring vertex isolation: the χ^2 of the B vertex must increase by more than half a unit when adding any other track in the event.

IV. DETERMINATION OF THE RATIO OF BRANCHING FRACTIONS

The ratio of the branching fractions is calculated from the number of signal candidates in the $B^0 \to K^{*0}\gamma$ and $B_s^0 \to \phi\gamma$ channels,

$$\frac{\mathcal{B}(B^0 \to K^{*0}\gamma)}{\mathcal{B}(B_s^0 \to \phi\gamma)} = \frac{N_{B^0\to K^{*0}\gamma}}{N_{B_s^0\to\phi\gamma}} \times \frac{\mathcal{B}(\phi \to K^+K^-)}{\mathcal{B}(K^{*0} \to K^+\pi^-)} \times \frac{f_s}{f_d} \times \frac{\epsilon_{B_s^0\to\phi\gamma}}{\epsilon_{B^0\to K^{*0}\gamma}}, \quad (1)$$

where N corresponds to the observed number of signal candidates (yield), $\mathcal{B}(\phi \to K^+K^-)$ and $\mathcal{B}(K^{*0} \to K^+\pi^-)$ are the visible branching fractions of the vector mesons, f_s/f_d is the ratio of the B^0 and B_s^0 hadronization fractions in pp collisions at $\sqrt{s} = 7$ TeV, and $\epsilon_{B_s^0\to\phi\gamma}/\epsilon_{B^0\to K^{*0}\gamma}$ is the ratio of efficiencies for the two decays. This latter ratio is split into contributions coming from the acceptance ($r_{\rm acc}$), the reconstruction and selection requirements ($r_{\rm reco}$), the PID requirements ($r_{\rm PID}$), and the trigger requirements ($r_{\rm trig}$),

$$\frac{\epsilon_{B_s^0\to\phi\gamma}}{\epsilon_{B^0\to K^{*0}\gamma}} = r_{\rm acc} \times r_{\rm reco} \times r_{\rm PID} \times r_{\rm trig}. \quad (2)$$

The PID efficiency ratio is measured from data to be $r_{\rm PID} = 0.787 \pm 0.010$(stat) by means of a calibration procedure using pure samples of kaons and pions from $D^{*\pm} \to D^0(K^+\pi^-)\pi^\pm$ decays selected utilizing purely kinematic criteria. The other efficiency ratios have been extracted using simulated events. The acceptance efficiency ratio $r_{\rm acc} = 1.094 \pm 0.004$(stat) exceeds unity because of the correlated acceptance of the kaons due to the limited phase space in the $\phi \to K^+K^-$ decay. These phase space constraints also cause the ϕ vertex to have a worse spatial resolution than the K^{*0} vertex. This affects the $B_s^0 \to \phi\gamma$ selection efficiency through the IP χ^2 and vertex isolation cuts while the common track cut $p_{\rm T} > 500$ MeV/c is less efficient on the softer pion from the K^{*0} decay. Both effects almost compensate and the reconstruction and selection efficiency ratio is found to be $r_{\rm reco} = 0.949 \pm 0.006$(stat), where the main systematic uncertainties in the numerator and denominator cancel since the kinematic selections are mostly identical for both decays. The trigger efficiency ratio $r_{\rm trig} = 1.057 \pm 0.008$(stat) has been computed taking into account the contributions from the different trigger configurations during the data taking period.

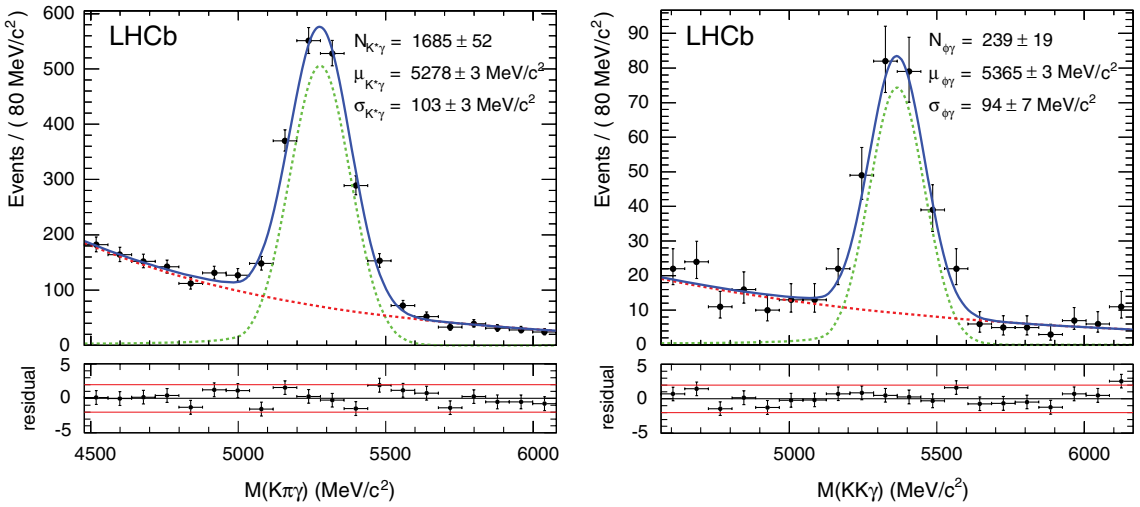

FIG. 1 (color online). Result of the fit for the $B^0 \to K^{*0}\gamma$ (left) and $B^0 s \to \phi\gamma$ (right). The black points represent the data, and the fit result is represented as a solid line. The signal is fitted with a Crystal Ball function (light, dashed-line) and the background is described as an exponential (dark, dashed-line). Below each invariant mass plot, the Poisson χ^2 residuals [19] are shown.

The yields of the two channels are extracted from a simultaneous unbinned maximum likelihood fit to the invariant mass distributions of the data. Signals are described using a Crystal Ball function [14], with the tail parameters fixed to their values extracted from MC simulation and the mass difference between the B^0 and B_s^0 signals fixed [15]. The width of the signal peak is left as a free parameter. Combinatorial background is parametrized by an exponential function with a different decay constant for each channel. The results of the fit are shown in Fig. 1. The number of events obtained for $B^0 \to K^{*0}\gamma$ and $B_s^0 \to \phi\gamma$ are 1685 ± 52 and 239 ± 19, with a signal over background ratio of $S/B = 3.1 \pm 0.4$ and 3.7 ± 1.3 in a $\pm 3\sigma$ window, respectively.

Several potential sources of peaking background have been studied: $B_{(s)}^0 \to K^+\pi^-\pi^0$ and $B_s^0 \to K^+K^-\pi^0$, where the two photons from the π^0 can be merged into a single cluster and misidentified as a single photon, $\Lambda_b^0 \to \Lambda^{*0}(Kp)\gamma$, where the proton can be misidentified as a pion or a kaon, and the irreducible $B_s^0 \to K^{*0}\gamma$. Their invariant-mass distributions and selection efficiencies have been evaluated from a sample of simulated events 10 times larger than the data and the number of predicted background events is determined and subtracted from the signal yield.

B decays in which one of the decay products has not been reconstructed, such as $B \to (K^{*0}\pi^0)X$ tend to accumulate towards lower values in the invariant mass distribution but can contaminate the signal peak. However, their contributions have not been included in the fit, and the correction to the fitted signal yield has been quantified by means of a statistical study. The mass distribution of the partially reconstructed B decays is first extracted from a sample of simulated events and the corresponding shape

TABLE I. Correction factors and corresponding uncertainties affecting the signal yields, in percent, induced by peaking backgrounds, partially reconstructed backgrounds, signal cross feed, and multiple candidates. The total uncertainty is obtained by summing the individual contributions in quadrature.

	$B^0 \to K^{*0}\gamma$		$B^0 s \to \phi\gamma$		Ratio	
Contribution	Correction	Error	Correction	Error	Correction	Error
$B^0 \to K^+\pi^-\pi^0$	-1.3	± 0.4	...	<0.1	-1.3	± 0.4
$B^0 s \to K^+\pi^-\pi^0$	-0.5	± 0.5	...	<0.1	-0.5	± 0.5
$B^0 s \to K^+K^-\pi^0$	...	<0.1	-1.3	± 1.3	$+1.3$	± 1.3
$\Lambda^0 b \to \Lambda^{*0}\gamma$	-0.7	± 0.2	-0.3	± 0.2	-0.4	± 0.3
$B^0 s \to K^{*0}\gamma$	-0.8	± 0.4	...	...	-0.8	± 0.4
Partially reconstructed B	$+0.04$	$^{+3.1}_{-0.2}$	$+4.5$	$^{+1.3}_{-2.9}$	-4.5	$^{+4.2}_{-1.3}$
$\phi\gamma/K^{*0}\gamma$ cross feed	-0.4	± 0.2	...	<0.1	-0.4	± 0.2
Multiple candidates	-0.5	± 0.2	-0.3	± 0.2	-0.2	± 0.3
Total	-4.2	$^{+3.2}_{-0.9}$	$+2.6$	$^{+1.9}_{-3.2}$	-6.8	$^{+4.5}_{-2.0}$

has been added to the fit with a free amplitude. The fit is then repeated many times, varying the shape parameters and the amplitude of the partially reconstructed component within their uncertainties. The correction to be applied to the signal yield and its uncertainty at a 95% confidence level are determined from the obtained distribution of the signal yield variation.

The effects of the cross feed between the two channels, i.e. $B^0 \to K^{*0}\gamma$ signal misidentified as $B_s^0 \to \phi\gamma$ and vice-versa, as well as the presence of multiple B candidates per event, have also been computed using simulation. The statistical uncertainty due to finite MC sample size is taken as the uncertainty in these corrections.

Table I summarizes all the corrections applied to the fitted signal yields, as well as the corresponding uncertainties for each source of background.

The ratio of branching fractions from Eq. (1) is calculated using the fitted yields of the signal corrected for the backgrounds, the values of the visible branching fractions [15], the LHCb measurement of f_s/f_d [16,17], and the values of the efficiency ratios described above. The result is

$$\frac{\mathcal{B}(B^0 \to K^{*0}\gamma)}{\mathcal{B}(B_s^0 \to \phi\gamma)} = 1.12 \pm 0.08(\text{stat}).$$

V. SYSTEMATIC UNCERTAINTIES

The limited size of the MC sample used in the calculation of r_{acc}, r_{reco}, and r_{trig} induces a systematic uncertainty in the ratio of branching fractions. In addition, r_{acc} is affected by uncertainties in the hadron reconstruction efficiency, arising from differences in the interaction of pions and kaons with the detector and the uncertainties in the description of the material of the detector. Differences in the mass window size of the vector mesons, combined with small differences in the position of the $K^{*0}(\phi)$ mass peaks between data and MC, produce a systematic uncertainty in r_{reco}, which has been evaluated by moving the center of the mass window to the value found in data. The reliability of the simulation to describe the IP χ^2 of the tracks and the B vertex isolation has been propagated into an uncertainty for r_{reco}. For this, the MC sample has been reweighted to reproduce the background-subtracted distributions from data, obtained by applying the *sPlot* technique [18] to separate signal and background components, using the invariant mass of the B candidate as the discriminant variable. No further systematic errors are associated with the use of MC simulation, since kinematic properties of the decays are known to be well-modeled. Systematic uncertainties associated with the photon are negligible due to the fact that its reconstruction in both decays is identical.

The systematic uncertainty associated with the PID calibration method has been evaluated using MC simulation. The statistical error due to the size of the kaon and pion calibration samples has also been propagated to r_{PID}.

TABLE II. Summary of contributions to the relative systematic uncertainty on the ratio of branching fractions. Note that f_s/f_d is quoted as a separate systematic uncertainty.

Source	Uncertainty (%)
Acceptance (r_{acc})	± 0.3
Selection (r_{reco})	± 1.4
PID efficiencies (r_{PID})	± 2.7
Trigger (r_{trig})	± 0.8
B mass window	± 0.9
Background	$^{+4.5}_{-2.0}$
Visible fraction of vector mesons	± 1.0
Quadratic sum of above	$^{+5.4}_{-3.3}$
f_s/f_d	$^{+7.9}_{-7.5}$

The systematic effect introduced by applying a B mass window cut of ± 800 MeV$/c^2$ has been evaluated by repeating the fit procedure with a tighter Bmass window reduced to ± 600 MeV$/c^2$.

Table II summarizes all sources of systematic uncertainty, including the background contributions detailed in Table I. The uncertainty on the ratio of efficiency-corrected yields is obtained by combining the individual sources in quadrature. The uncertainty on the ratio f_s/f_d is given as a separate source of uncertainty.

Besides f_s/f_d, the dominant source of systematic uncertainty is the imperfect modelling of the backgrounds due to partially reconstructed B decays. This specific uncertainty is expected to be reduced when more data are available.

VI. RESULTS AND CONCLUSIONS

In 0.37 fb^{-1} of pp collisions at a center of mass energy of $\sqrt{s} = 7$ TeV the ratio of branching fractions of $B^0 \to K^{*0}\gamma$ and $B_s^0 \to \phi\gamma$ decays has been measured to be

$$\frac{\mathcal{B}(B^0 \to K^{*0}\gamma)}{\mathcal{B}(B_s^0 \to \phi\gamma)} = 1.12 \pm 0.08(\text{stat})^{+0.06}_{-0.04}(\text{syst})^{+0.09}_{-0.08}(f_s/f_d)$$

in good agreement with the theoretical prediction of 1.0 ± 0.2 [6].

Using $\mathcal{B}(B^0 \to K^{*0}\gamma) = (4.33 \pm 0.15) \times 10^{-5}$ [4], one obtains

$$\mathcal{B}(B_s^0 \to \phi\gamma) = (3.9 \pm 0.5) \times 10^{-5}$$

(statistical and systematic errors combined), which agrees with the previous experimental value. This is the most precise measurement of the $B_s^0 \to \phi\gamma$ branching fraction to date.

ACKNOWLEDGMENTS

We express our gratitude to our colleagues in the CERN accelerator departments for the excellent performance of

the LHC. We thank the technical and administrative staff at CERN and at the LHCb institutes, and acknowledge support from the National Agencies: CAPES, CNPq, FAPERJ, and FINEP (Brazil); CERN; NSFC (China); CNRS-IN2P3 (France); BMBF, DFG, HGF and MPG (Germany); SFI (Ireland); INFN (Italy); FOM and NWO (The Netherlands); SCSR (Poland); ANCS (Romania); MinES of Russia and Rosatom (Russia); MICINN, XuntaGal and GENCAT (Spain); SNSF and SER (Switzerland); NAS Ukraine (Ukraine); STFC (United Kingdom); NSF (USA). We also acknowledge support received from the ERC under FP7 and the Region Auvergne.

[1] S. Descotes-Genon, D. Ghosh, J. Matias, and M. Ramon, J. High Energy Phys. 06 (2011) 099; T. Gershon and A. Soni, J. Phys. G **34**, 479 (2007); F. Mahmoudi and M. R. Ahmady, AIP Conf. Proc. **903**, 283 (2007); W. Altmannshofer, P. Paradisi, and D. M. Straub, J. High Energy Phys. 04 (2012) 008.
[2] R. Ammar *et al.* (CLEO Collaboration), Phys. Rev. Lett. **71**, 674 (1993).
[3] J. Wicht *et al.* (Belle Collaboration), Phys. Rev. Lett. **100**, 121801 (2008).
[4] D. Asner *et al.* (Heavy Flavor Averaging Group), arXiv:1010.1589.
[5] B. Aubert *et al.* (*BABAR* Collaboration), Phys. Rev. Lett. **103**, 211802 (2009). M. Nakao *et al.* (Belle Collaboration), Phys. Rev. D **69**, 112001 (2004).T. E. Coan *et al.* (CLEO Collaboration), Phys. Rev. Lett. **84**, 5283 (2000).
[6] A. Ali, B. D. Pecjak, and C. Greub, Eur. Phys. J. C **55**, 577 (2008).
[7] A. Augusto Alves, Jr. *et al.* (LHCb Collaboration), JINST **3**, S08005 (2008).
[8] M. Clemencic, G. Corti, S. Easo, C. R. Jones, S. Miglioranzi, M. Pappagallo, and P. Robbe, J. Phys. Conf. Ser. **331**, 032023 (2011).
[9] T. Sjöstrand, S. Mrenna, and P. Skands, J. High Energy Phys. 05 (2006) 026.
[10] D. J. Lange, Nucl. Instrum. Methods Phys. Res., Sect. A **462**, 152 (2001).
[11] E. Barberio and Z. Was, Comput. Phys. Commun. **79**, 291 (1994).
[12] S. Agostinelli *et al.*, Nucl. Instrum. Methods Phys. Res., Sect. A **506**, 250 (2003).
[13] O. Deschamps, F. Machefert, M.-H. Schune, G. Pakhlova, and I. Belyaev, LHCb-2003-091.
[14] T. Skwarnicki, Ph.D. thesis, Cracow Institute of Nuclear Physics, 1986 [Report No. DESY-F31-86-02].
[15] K. Nakamura *et al.* (Particle Data Group), J. Phys. G **37**, 075021 (2010).
[16] R. Aaij *et al.* (LHCb Collaboration), Phys. Rev. Lett. **107**, 211801 (2011).
[17] R. Aaij *et al.* (LHCb Collaboration), Phys. Rev. D **85**, 032008 (2012).
[18] M. Pivk and F. R. Le Diberder, Nucl. Instrum. Methods Phys. Res., Sect. A **555**, 356 (2005).
[19] S. Baker and R. D. Cousins, Nucl. Instrum. Methods Phys. Res., Sect. A **221**, 437 (1984).

R. Aaij,[38] C. Abellan Beteta,[33,n] B. Adeva,[34] M. Adinolfi,[43] C. Adrover,[6] A. Affolder,[49] Z. Ajaltouni,[5] J. Albrecht,[35] F. Alessio,[35] M. Alexander,[48] G. Alkhazov,[27] P. Alvarez Cartelle,[34] A. A. Alves, Jr.,[22] S. Amato,[2] Y. Amhis,[36] J. Anderson,[37] R. B. Appleby,[51] O. Aquines Gutierrez,[10] F. Archilli,[18,35] L. Arrabito,[55] A. Artamonov,[32] M. Artuso,[53,35] E. Aslanides,[6] G. Auriemma,[22,m] S. Bachmann,[11] J. J. Back,[45] D. S. Bailey,[51] V. Balagura,[28,35] W. Baldini,[16] R. J. Barlow,[51] C. Barschel,[35] S. Barsuk,[7] W. Barter,[44] A. Bates,[48] C. Bauer,[10] Th. Bauer,[38] A. Bay,[36] I. Bediaga,[1] S. Belogurov,[28] K. Belous,[32] I. Belyaev,[28] E. Ben-Haim,[8] M. Benayoun,[8] G. Bencivenni,[18] S. Benson,[47] J. Benton,[43] R. Bernet,[37] M.-O. Bettler,[17] M. van Beuzekom,[38] A. Bien,[11] S. Bifani,[12] T. Bird,[51] A. Bizzeti,[17,h] P. M. Bjørnstad,[51] T. Blake,[35] F. Blanc,[36] C. Blanks,[50] J. Blouw,[11] S. Blusk,[53] A. Bobrov,[31] V. Bocci,[22] A. Bondar,[31] N. Bondar,[27] W. Bonivento,[15] S. Borghi,[48,51] A. Borgia,[53] T. J. V. Bowcock,[49] C. Bozzi,[16] T. Brambach,[9] J. van den Brand,[39] J. Bressieux,[36] D. Brett,[51] M. Britsch,[10] T. Britton,[53] N. H. Brook,[43] H. Brown,[49] A. Büchler-Germann,[37] I. Burducea,[26] A. Bursche,[37] J. Buytaert,[35] S. Cadeddu,[15] O. Callot,[7] M. Calvi,[20,j] M. Calvo Gomez,[33,n] A. Camboni,[33] P. Campana,[18,35] A. Carbone,[14] G. Carboni,[21,k] R. Cardinale,[19,35,i] A. Cardini,[15] L. Carson,[50] K. Carvalho Akiba,[2] G. Casse,[49] M. Cattaneo,[35] Ch. Cauet,[9] M. Charles,[52] Ph. Charpentier,[35] N. Chiapolini,[37] K. Ciba,[35] X. Cid Vidal,[34] G. Ciezarek,[50] P. E. L. Clarke,[47,35] M. Clemencic,[35] H. V. Cliff,[44] J. Closier,[35] C. Coca,[26] V. Coco,[38] J. Cogan,[6] P. Collins,[35] A. Comerma-Montells,[33] F. Constantin,[26] A. Contu,[52] A. Cook,[43] M. Coombes,[43] G. Corti,[35] B. Couturier,[35] G. A. Cowan,[36] R. Currie,[47] C. D'Ambrosio,[35] P. David,[8] P. N. Y. David,[38] I. De Bonis,[4] K. De Bruyn,[38] S. De Capua,[21,k] M. De Cian,[37] F. De Lorenzi,[12] J. M. De Miranda,[1] L. De Paula,[2] P. De Simone,[18] D. Decamp,[4] M. Deckenhoff,[9] H. Degaudenzi,[36,35] L. Del Buono,[8] C. Deplano,[15] D. Derkach,[14,35] O. Deschamps,[5] F. Dettori,[39] J. Dickens,[44] H. Dijkstra,[35] P. Diniz Batista,[1] F. Domingo Bonal,[33,n]

S. Donleavy,[49] F. Dordei,[11] A. Dosil Suárez,[34] D. Dossett,[45] A. Dovbnya,[40] F. Dupertuis,[36] R. Dzhelyadin,[32] A. Dziurda,[23] S. Easo,[46] U. Egede,[50] V. Egorychev,[28] S. Eidelman,[31] D. van Eijk,[38] F. Eisele,[11] S. Eisenhardt,[47] R. Ekelhof,[9] L. Eklund,[48] Ch. Elsasser,[37] D. Elsby,[42] D. Esperante Pereira,[34] A. Falabella,[16,14,e] E. Fanchini,[20,j] C. Färber,[11] G. Fardell,[47] C. Farinelli,[38] S. Farry,[12] V. Fave,[36] V. Fernandez Albor,[34] M. Ferro-Luzzi,[35] S. Filippov,[30] C. Fitzpatrick,[47] M. Fontana,[10] F. Fontanelli,[19,i] R. Forty,[35] O. Francisco,[2] M. Frank,[35] C. Frei,[35] M. Frosini,[17,f] S. Furcas,[20] A. Gallas Torreira,[34] D. Galli,[14,c] M. Gandelman,[2] P. Gandini,[52] Y. Gao,[3] J.-C. Garnier,[35] J. Garofoli,[53] J. Garra Tico,[44] L. Garrido,[33] D. Gascon,[33] C. Gaspar,[35] R. Gauld,[52] N. Gauvin,[36] M. Gersabeck,[35] T. Gershon,[45,35] Ph. Ghez,[4] V. Gibson,[44] V. V. Gligorov,[35] C. Göbel,[54] D. Golubkov,[28] A. Golutvin,[50,28,35] A. Gomes,[2] H. Gordon,[52] M. Grabalosa Gándara,[33] R. Graciani Diaz,[33] L. A. Granado Cardoso,[35] E. Graugés,[33] G. Graziani,[17] A. Grecu,[26] E. Greening,[52] S. Gregson,[44] B. Gui,[53] E. Gushchin,[30] Yu. Guz,[32] T. Gys,[35] C. Hadjivasiliou,[53] G. Haefeli,[36] C. Haen,[35] S. C. Haines,[44] T. Hampson,[43] S. Hansmann-Menzemer,[11] R. Harji,[50] N. Harnew,[52] J. Harrison,[51] P. F. Harrison,[45] T. Hartmann,[56] J. He,[7] V. Heijne,[38] K. Hennessy,[49] P. Henrard,[5] J. A. Hernando Morata,[34] E. van Herwijnen,[35] E. Hicks,[49] K. Holubyev,[11] P. Hopchev,[4] W. Hulsbergen,[38] P. Hunt,[52] T. Huse,[49] R. S. Huston,[12] D. Hutchcroft,[49] D. Hynds,[48] V. Iakovenko,[41] P. Ilten,[12] J. Imong,[43] R. Jacobsson,[35] A. Jaeger,[11] M. Jahjah Hussein,[5] E. Jans,[38] F. Jansen,[38] P. Jaton,[36] B. Jean-Marie,[7] F. Jing,[3] M. John,[52] D. Johnson,[52] C. R. Jones,[44] B. Jost,[35] M. Kaballo,[9] S. Kandybei,[40] M. Karacson,[35] T. M. Karbach,[9] J. Keaveney,[12] I. R. Kenyon,[42] U. Kerzel,[35] T. Ketel,[39] A. Keune,[36] B. Khanji,[6] Y. M. Kim,[47] M. Knecht,[36] R. F. Koopman,[39] P. Koppenburg,[38] M. Korolev,[29] A. Kozlinskiy,[38] L. Kravchuk,[30] K. Kreplin,[11] M. Kreps,[45] G. Krocker,[11] P. Krokovny,[11] F. Kruse,[9] K. Kruzelecki,[35] M. Kucharczyk,[20,23,35,j] T. Kvaratskheliya,[28,35] V. N. La Thi,[36] D. Lacarrere,[35] G. Lafferty,[51] A. Lai,[15] D. Lambert,[47] R. W. Lambert,[39] E. Lanciotti,[35] G. Lanfranchi,[18] C. Langenbruch,[11] T. Latham,[45] C. Lazzeroni,[42] R. Le Gac,[6] J. van Leerdam,[38] J.-P. Lees,[4] R. Lefèvre,[5] A. Leflat,[29,35] J. Lefrançois,[7] O. Leroy,[6] T. Lesiak,[23] L. Li,[3] L. Li Gioi,[5] M. Lieng,[9] M. Liles,[49] R. Lindner,[35] C. Linn,[11] B. Liu,[3] G. Liu,[35] J. von Loeben,[20] J. H. Lopes,[2] E. Lopez Asamar,[33] N. Lopez-March,[36] H. Lu,[3] J. Luisier,[36] A. Mac Raighne,[48] F. Machefert,[7] I. V. Machikhiliyan,[4,28] F. Maciuc,[10] O. Maev,[27,35] J. Magnin,[1] S. Malde,[52] R. M. D. Mamunur,[35] G. Manca,[15,d] G. Mancinelli,[6] N. Mangiafave,[44] U. Marconi,[14] R. Märki,[36] J. Marks,[11] G. Martellotti,[22] A. Martens,[8] L. Martin,[52] A. Martín Sánchez,[7] D. Martinez Santos,[35] A. Massafferri,[1] Z. Mathe,[12] C. Matteuzzi,[20] M. Matveev,[27] E. Maurice,[6] B. Maynard,[53] A. Mazurov,[16,30,35] G. McGregor,[51] R. McNulty,[12] M. Meissner,[11] M. Merk,[38] J. Merkel,[9] R. Messi,[21,k] S. Miglioranzi,[35] D. A. Milanes,[13] M.-N. Minard,[4] J. Molina Rodriguez,[54] S. Monteil,[5] D. Moran,[12] P. Morawski,[23] R. Mountain,[53] I. Mous,[38] F. Muheim,[47] K. Müller,[37] R. Muresan,[26] B. Muryn,[24] B. Muster,[36] M. Musy,[33] J. Mylroie-Smith,[49] P. Naik,[43] T. Nakada,[36] R. Nandakumar,[46] I. Nasteva,[1] M. Nedos,[9] M. Needham,[47] N. Neufeld,[35] A. D. Nguyen,[36] C. Nguyen-Mau,[36,o] M. Nicol,[7] V. Niess,[5] N. Nikitin,[29] T. Nikodem,[11] A. Nomerotski,[52,35] A. Novoselov,[32] A. Oblakowska-Mucha,[24] V. Obraztsov,[32] S. Oggero,[38] S. Ogilvy,[48] O. Okhrimenko,[41] R. Oldeman,[15,35,d] M. Orlandea,[26] J. M. Otalora Goicochea,[2] P. Owen,[50] B. K. Pal,[53] J. Palacios,[37] A. Palano,[13,b] M. Palutan,[18] J. Panman,[35] A. Papanestis,[46] M. Pappagallo,[48] C. Parkes,[51] C. J. Parkinson,[50] G. Passaleva,[17] G. D. Patel,[49] M. Patel,[50] S. K. Paterson,[50] G. N. Patrick,[46] C. Patrignani,[19,i] C. Pavel-Nicorescu,[26] A. Pazos Alvarez,[34] A. Pellegrino,[38] G. Penso,[22,l] M. Pepe Altarelli,[35] S. Perazzini,[14,c] D. L. Perego,[20,j] E. Perez Trigo,[34] A. Pérez-Calero Yzquierdo,[33] P. Perret,[5] M. Perrin-Terrin,[6] G. Pessina,[20] A. Petrella,[16,35] A. Petrolini,[19,i] A. Phan,[53] E. Picatoste Olloqui,[33] B. Pie Valls,[33] B. Pietrzyk,[4] T. Pilař,[45] D. Pinci,[22] R. Plackett,[48] S. Playfer,[47] M. Plo Casasus,[34] G. Polok,[23] A. Poluektov,[45,31] E. Polycarpo,[2] D. Popov,[10] B. Popovici,[26] C. Potterat,[33] A. Powell,[52] J. Prisciandaro,[36] V. Pugatch,[41] A. Puig Navarro,[33] W. Qian,[53] J. H. Rademacker,[43] B. Rakotomiaramanana,[36] M. S. Rangel,[2] I. Raniuk,[40] G. Raven,[39] S. Redford,[52] M. M. Reid,[45] A. C. dos Reis,[1] S. Ricciardi,[46] A. Richards,[50] K. Rinnert,[49] D. A. Roa Romero,[5] P. Robbe,[7] E. Rodrigues,[48,51] F. Rodrigues,[2] P. Rodriguez Perez,[34] G. J. Rogers,[44] S. Roiser,[35] V. Romanovsky,[32] M. Rosello,[33,n] J. Rouvinet,[36] T. Ruf,[35] H. Ruiz,[33] G. Sabatino,[21,k] J. J. Saborido Silva,[34] N. Sagidova,[27] P. Sail,[48] B. Saitta,[15,d] C. Salzmann,[37] M. Sannino,[19,i] R. Santacesaria,[22] C. Santamarina Rios,[34] R. Santinelli,[35] E. Santovetti,[21,k] M. Sapunov,[6] A. Sarti,[18,l] C. Satriano,[22,m] A. Satta,[21] M. Savrie,[16,e] D. Savrina,[28] P. Schaack,[50] M. Schiller,[39] S. Schleich,[9] M. Schlupp,[9] M. Schmelling,[10] B. Schmidt,[35] O. Schneider,[36] A. Schopper,[35] M.-H. Schune,[7] R. Schwemmer,[35] B. Sciascia,[18] A. Sciubba,[18,l] M. Seco,[34] A. Semennikov,[28] K. Senderowska,[24] I. Sepp,[50] N. Serra,[37] J. Serrano,[6] P. Seyfert,[11] M. Shapkin,[32] I. Shapoval,[40,35] P. Shatalov,[28] Y. Shcheglov,[27] T. Shears,[49] L. Shekhtman,[31] O. Shevchenko,[40] V. Shevchenko,[28] A. Shires,[50] R. Silva Coutinho,[45] T. Skwarnicki,[53] N. A. Smith,[49] E. Smith,[52,46] K. Sobczak,[5] F. J. P. Soler,[48] A. Solomin,[43] F. Soomro,[18,35] B. Souza De Paula,[2] B. Spaan,[9] A. Sparkes,[47] P. Spradlin,[48] F. Stagni,[35]

S. Stahl,[11] O. Steinkamp,[37] S. Stoica,[26] S. Stone,[53,35] B. Storaci,[38] M. Straticiuc,[26] U. Straumann,[37] V. K. Subbiah,[35] S. Swientek,[9] M. Szczekowski,[25] P. Szczypka,[36] T. Szumlak,[24] S. T'Jampens,[4] E. Teodorescu,[26] F. Teubert,[35] C. Thomas,[52] E. Thomas,[35] J. van Tilburg,[11] V. Tisserand,[4] M. Tobin,[37] S. Tolk,[39] S. Topp-Joergensen,[52] N. Torr,[52] E. Tournefier,[4,50] S. Tourneur,[36] M. T. Tran,[36] A. Tsaregorodtsev,[6] N. Tuning,[38] M. Ubeda Garcia,[35] A. Ukleja,[25] P. Urquijo,[53] U. Uwer,[11] V. Vagnoni,[14] G. Valenti,[14] R. Vazquez Gomez,[33] P. Vazquez Regueiro,[34] S. Vecchi,[16] J. J. Velthuis,[43] M. Veltri,[17,g] B. Viaud,[7] I. Videau,[7] D. Vieira,[2] X. Vilasis-Cardona,[33,n] J. Visniakov,[34] A. Vollhardt,[37] D. Volyanskyy,[10] D. Voong,[43] A. Vorobyev,[27] H. Voss,[10] S. Wandernoth,[11] J. Wang,[53] D. R. Ward,[44] N. K. Watson,[42] A. D. Webber,[51] D. Websdale,[50] M. Whitehead,[45] D. Wiedner,[11] L. Wiggers,[38] G. Wilkinson,[52] M. P. Williams,[45,46] M. Williams,[50] F. F. Wilson,[46] J. Wishahi,[9] M. Witek,[23] W. Witzeling,[35] S. A. Wotton,[44] K. Wyllie,[35] Y. Xie,[47] F. Xing,[52] Z. Xing,[53] Z. Yang,[3] R. Young,[47] O. Yushchenko,[32] M. Zangoli,[14] M. Zavertyaev,[10,a] F. Zhang,[3] L. Zhang,[53] W. C. Zhang,[12] Y. Zhang,[3] A. Zhelezov,[11] L. Zhong,[3] and A. Zvyagin[35]

(LHCb Collaboration)

[1]*Centro Brasileiro de Pesquisas Físicas (CBPF), Rio de Janeiro, Brazil*
[2]*Universidade Federal do Rio de Janeiro (UFRJ), Rio de Janeiro, Brazil*
[3]*Center for High Energy Physics, Tsinghua University, Beijing, China*
[4]*LAPP, Université de Savoie, CNRS/IN2P3, Annecy-Le-Vieux, France*
[5]*Clermont Université, Université Blaise Pascal, CNRS/IN2P3, LPC, Clermont-Ferrand, France*
[6]*CPPM, Aix-Marseille Université, CNRS/IN2P3, Marseille, France*
[7]*LAL, Université Paris-Sud, CNRS/IN2P3, Orsay, France*
[8]*LPNHE, Université Pierre et Marie Curie, Université Paris Diderot, CNRS/IN2P3, Paris, France*
[9]*Fakultät Physik, Technische Universität Dortmund, Dortmund, Germany*
[10]*Max-Planck-Institut für Kernphysik (MPIK), Heidelberg, Germany*
[11]*Physikalisches Institut, Ruprecht-Karls-Universität Heidelberg, Heidelberg, Germany*
[12]*School of Physics, University College Dublin, Dublin, Ireland*
[13]*Sezione INFN di Bari, Bari, Italy*
[14]*Sezione INFN di Bologna, Bologna, Italy*
[15]*Sezione INFN di Cagliari, Cagliari, Italy*
[16]*Sezione INFN di Ferrara, Ferrara, Italy*
[17]*Sezione INFN di Firenze, Firenze, Italy*
[18]*Laboratori Nazionali dell'INFN di Frascati, Frascati, Italy*
[19]*Sezione INFN di Genova, Genova, Italy*
[20]*Sezione INFN di Milano Bicocca, Milano, Italy*
[21]*Sezione INFN di Roma Tor Vergata, Roma, Italy*
[22]*Sezione INFN di Roma La Sapienza, Roma, Italy*
[23]*Henryk Niewodniczanski Institute of Nuclear Physics Polish Academy of Sciences, Kraków, Poland*
[24]*AGH University of Science and Technology, Kraków, Poland*
[25]*Soltan Institute for Nuclear Studies, Warsaw, Poland*
[26]*Horia Hulubei National Institute of Physics and Nuclear Engineering, Bucharest-Magurele, Romania*
[27]*Petersburg Nuclear Physics Institute (PNPI), Gatchina, Russia*
[28]*Institute of Theoretical and Experimental Physics (ITEP), Moscow, Russia*
[29]*Institute of Nuclear Physics, Moscow State University (SINP MSU), Moscow, Russia*
[30]*Institute for Nuclear Research of the Russian Academy of Sciences (INR RAN), Moscow, Russia*
[31]*Budker Institute of Nuclear Physics (SB RAS) and Novosibirsk State University, Novosibirsk, Russia*
[32]*Institute for High Energy Physics (IHEP), Protvino, Russia*
[33]*Universitat de Barcelona, Barcelona, Spain*
[34]*Universidad de Santiago de Compostela, Santiago de Compostela, Spain*
[35]*European Organization for Nuclear Research (CERN), Geneva, Switzerland*
[36]*Ecole Polytechnique Fédérale de Lausanne (EPFL), Lausanne, Switzerland*
[37]*Physik-Institut, Universität Zürich, Zürich, Switzerland*
[38]*Nikhef National Institute for Subatomic Physics, Amsterdam, The Netherlands*
[39]*Nikhef National Institute for Subatomic Physics and Vrije Universiteit, Amsterdam, The Netherlands*
[40]*NSC Kharkiv Institute of Physics and Technology (NSC KIPT), Kharkiv, Ukraine*
[41]*Institute for Nuclear Research of the National Academy of Sciences (KINR), Kyiv, Ukraine*
[42]*University of Birmingham, Birmingham, United Kingdom*
[43]*H. H. Wills Physics Laboratory, University of Bristol, Bristol, United Kingdom*
[44]*Cavendish Laboratory, University of Cambridge, Cambridge, United Kingdom*

[45]*Department of Physics, University of Warwick, Coventry, United Kingdom*
[46]*STFC Rutherford Appleton Laboratory, Didcot, United Kingdom*
[47]*School of Physics and Astronomy, University of Edinburgh, Edinburgh, United Kingdom*
[48]*School of Physics and Astronomy, University of Glasgow, Glasgow, United Kingdom*
[49]*Oliver Lodge Laboratory, University of Liverpool, Liverpool, United Kingdom*
[50]*Imperial College London, London, United Kingdom*
[51]*School of Physics and Astronomy, University of Manchester, Manchester, United Kingdom*
[52]*Department of Physics, University of Oxford, Oxford, United Kingdom*
[53]*Syracuse University, Syracuse, New York, USA*
[54]*Pontifícia Universidade Católica do Rio de Janeiro (PUC-Rio), Rio de Janeiro, Brazil, associated to Universidade Federal do Rio de Janeiro (UFRJ), Rio de Janeiro, Brazil*
[55]*CC-IN2P3, CNRS-IN2P3, Lyon-Villeurbanne, France, associated member*
[56]*Physikalisches Institut, Universität Rostock, Rostock, Germany, associated to Physikalisches Institut, Ruprecht-Karls-Universität Heidelberg, Heidelberg, Germany*

[a]Also at P. N. Lebedev Physical Institute, Russian Academy of Science (LPI RAS), Moscow, Russia.
[b]Also at Università di Bari, Bari, Italy.
[c]Also at Università di Bologna, Bologna, Italy.
[d]Also at Università di Cagliari, Cagliari, Italy.
[e]Also at Università di Ferrara, Ferrara, Italy.
[f]Also at Università di Firenze, Firenze, Italy.
[g]Also at Università di Urbino, Urbino, Italy.
[h]Also at Università di Modena e Reggio Emilia, Modena, Italy.
[i]Also at Università di Genova, Genova, Italy.
[j]Also at Università di Milano Bicocca, Milano, Italy.
[k]Also at Università di Roma Tor Vergata, Roma, Italy.
[l]Also at Università di Roma La Sapienza, Roma, Italy.
[m]Also at Università della Basilicata, Potenza, Italy.
[n]Also at LIFAELS, La Salle, Universitat Ramon Llull, Barcelona, Spain.
[o]Also at Hanoi University of Science, Hanoi, Vietnam.